

# Photonic material for designing arbitrarily shaped mirrors and microcavities in two dimensions

|                              |   |
|------------------------------|---|
| 著者                           | 宮崎 博司   |
| journal or publication title | Journal of applied physics  |
| volume                       | 95  |
| number                       | 9   |
| page range                   | 4555-4558   |
| year                         | 2004  |
| URL                          | <a href="http://hdl.handle.net/10097/35681">http://hdl.handle.net/10097/35681</a> |

doi: 10.1063/1.1691484

# Photonic material for designing arbitrarily shaped mirrors and microcavities in two dimensions

Hiroshi Miyazaki<sup>a)</sup>

*Department of Applied Physics, Tohoku University, Aramaki, Sendai 980-8579, Japan*

Masashi Hase

*National Institute for Materials Science (NIMS), 1-2-1 Sengen, Tsukuba 305-0047, Japan*

Hideki T. Miyazaki

*National Institute for Materials Science (NIMS), 1-2-1 Sengen, Tsukuba 305-0047, Japan*

Yoichi Kurokawa

*Department of Applied Physics, Tohoku University, Aramaki, Sendai 980-8579, Japan*

Norio Shinya

*National Institute for Materials Science (NIMS), 1-2-1 Sengen, Tsukuba 305-0047, Japan*

(Received 7 November 2003; accepted 10 February 2004)

Based on the numerical finding of a two-dimensional photonic material which has large complete photonic gaps and structural uniformity, we propose a photonic plate which can be used to design arbitrarily shaped photonic mirrors and microcavities on a wavelength scale. This paper describes a wavelength-sized parabolic mirror that can collect light very efficiently without loss. In addition, we present circular microcavities of tunable resonance frequencies with high values of quality factor  $Q$ .

© 2004 American Institute of Physics. [DOI: 10.1063/1.1691484]

## I. INTRODUCTION

Photonic crystals (PhC's) are artificial photonic materials whose periodic structure engenders photonic gaps (PG's), ranges of frequencies at which light cannot propagate within the PhC's. Using these PG's, PhC's can be used to confine or guide light within the wavelength scale. Their increased use is anticipated for wide technological applications in the near future.<sup>1-3</sup> One example is an optical waveguide, which is ordinarily formed by removing periodic elements along a certain line. Consequently, its structure should be commensurate with the periodicity of the host PhC. This characteristic is different from the conventional waveguides of microwaves, which are made of metal plates. Metals can reflect microwaves of arbitrary incidence angle without loss. Therefore optical materials that have both complete PG and structural flexibility in the wavelength scale are necessary to create such an arbitrarily shaped waveguide in the optical region.

We recently proposed a two-dimensional photonic material: uniformly distributed photonic scatterers (UDPS's).<sup>4</sup> UDPS's are formed by randomly placing parallel dielectric rods under the condition that distance  $|\mathbf{R}_i - \mathbf{R}_j|$  between the centers of  $i$ th and  $j$ th rods,  $\mathbf{R}_i$  and  $\mathbf{R}_j$ , is larger than a certain value  $D_{\min}$ , i.e.,  $|\mathbf{R}_i - \mathbf{R}_j| > D_{\min}$ . When rods have sufficient density and dielectric contrast, UDPS's have large complete PG's. Our study also demonstrated the highly efficient transmission of light in arbitrarily shaped waveguides that is comparable with wavelength  $\lambda$ . Such efficiency is achieved by combining UDPS's and smooth sidewalls made of periodic rods. The present study shows that combined use of UDPS's

and sidewalls, which we call a UDPS plate, enables us to design two-dimensional curved mirrors and microcavities of arbitrary shape whose size can be reduced to the wavelength order.

## II. UDPS PLATES

Figure 1(a) shows an example of UDPS's plates. Periodic rods of radius  $a$  and dielectric constant  $\epsilon=12$  surround a rectangular region of  $|x| < 80a$  and  $-26.67a < y < 0$ . Each rod is represented by a white circle. Then, we fill the surrounded region with UDPS's. We generate more than one million random sets of rod positions within the rectangular region and place rods successively so that the distances between a rod and those already placed are always greater than  $D_{\min}$ . This procedure yields extremely uniform and dense rod distribution if the number of randomly generated rod positions is sufficiently large. In this study, we commonly choose  $D_{\min}=4a$ . Transmittance  $T$  is obtained for plane-wave incidence of the TM or TE ( $\mathbf{E}$  or  $\mathbf{H} \parallel$  rod axis) mode from the positive  $y$  axis by calculating the energy flow at the line  $L$  using the multiple-scattering method.<sup>5</sup>

Average transmittances over five rod configurations including Fig. 1(a) are shown by blue (TM) and red (TE) lines in Fig. 1(c) as a function of size parameter  $\Omega = 2\pi a/\lambda$ . Adopting the gap condition as  $|T| < 0.01$ , we find the PG of the TM mode as  $0.362 < \Omega < 0.508$  with average penetration depth of about  $2a$ . The PG of the TE mode is  $0.732 < \Omega < 0.782$ . Figure 1(a) shows distributions of total electric-field intensity and energy flow (white arrows) for the TM mode incidence at  $\Omega=0.40$  ( $\lambda = 15.71a$ ). One can see the yellow-red region of large intensity lying parallel to the upper sidewall. Its periodicity equals the wavelength. Therefore the

<sup>a)</sup>Electronic mail: hmiyazak@olive.apph.tohoku.ac.jp

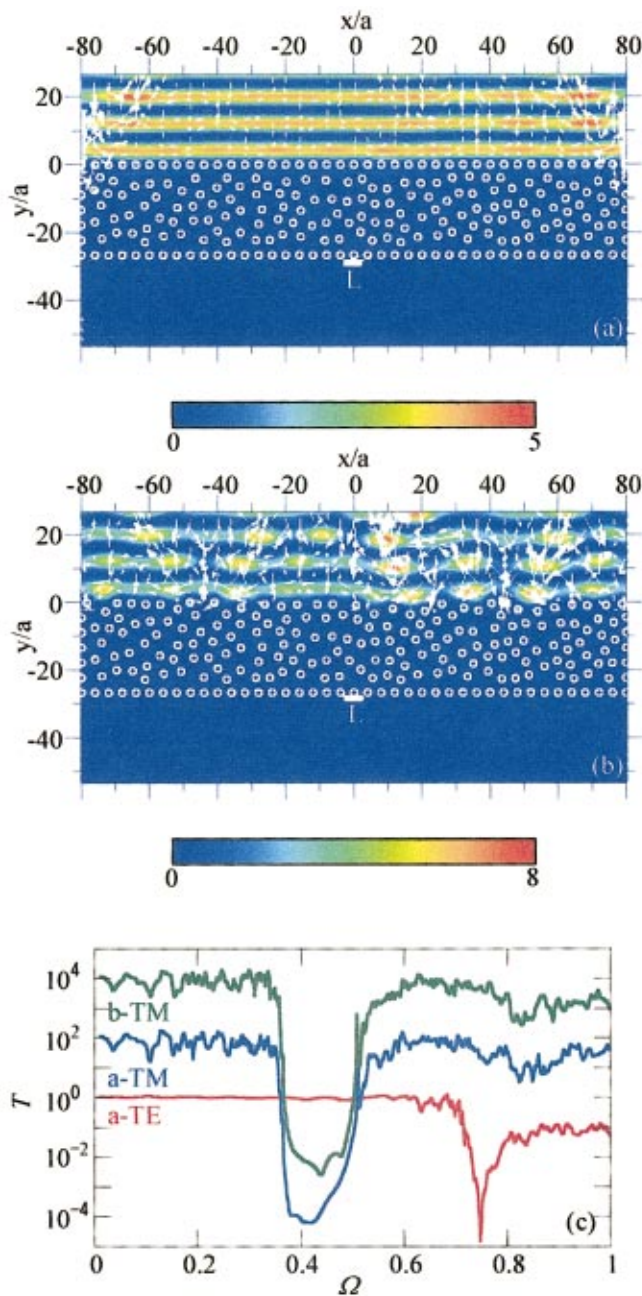


FIG. 1. (Color) (a), (b) Examples of UDPS plates. In (a), dielectric rods of radius  $a$  and  $\epsilon=12$  are arranged periodically within the vacuum as sidewalls along the rectangular region of  $|x|<80a$  and  $-26.67a<y<0$ , whereas the upper sidewall is removed in (b). Their periods are  $4.0a$  and  $4.44a$  along the  $x$  and  $y$  axes, respectively. The rectangle interior is filled with rods satisfying the condition that rod distance be larger than  $D_{\min}=4a$ . Volume fractions  $V_f$  are 0.174 and 0.164 in (a) and (b), respectively. Distributions are also shown of the total electric field intensity and energy flow (white arrows) at  $\Omega=0.40$  for the TM mode incidence of the plane wave from the positive  $y$  axis. Intensity increases from blue to red with maxima of 4.73 and 7.53 in (a) and (b), respectively. (c) Transmittance as a function of size parameter  $\Omega=2\pi a/\lambda$  at the line  $L$  of length  $5.67a$  placed at  $y=-28.17a$ . The plane wave of the TM or TE mode is incident from the positive  $y$  axis. Transmittance is the average of five configurations including (a) or (b).

UDPS plate in Fig. 1(a) can be regarded as an ideal flat mirror without loss. Detailed calculation reveals that we can effectively replace this UDPS plate with a perfectly reflecting flat mirror at  $y=0.7a$ .

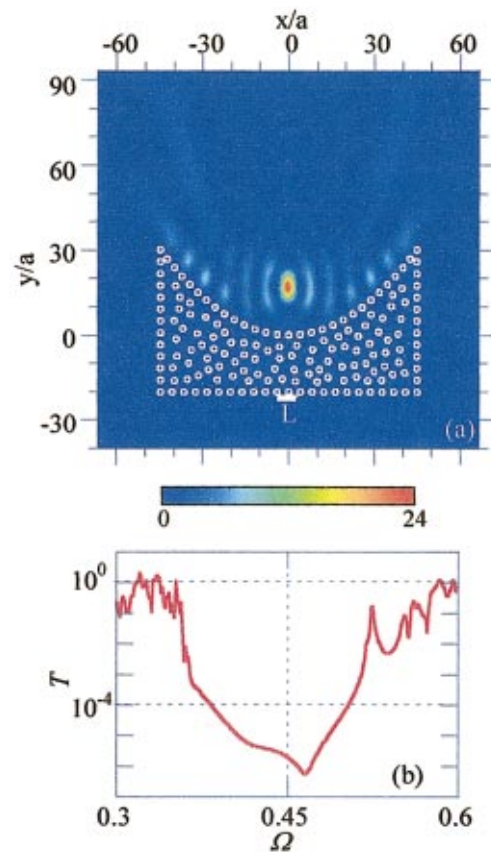


FIG. 2. (Color) (a) Parabola mirror made of the UDPS plate. (b) Transmittance of the TM mode at line  $L$ . Plane wave of the TM mode is incident from the positive  $y$  axis. Rods are placed along the rectangular region of  $|x|<44.80a$  and  $-20a<y<30.13a$ . The lower and right or left sidewalls are made with period  $4.07a$  and  $4.59a$ , respectively. The upper sidewall is formed by putting rods with period  $4a$  along the parabola  $y=x^2/4f$  with  $f=16.67a$ . The volume fraction  $V_f$  is 0.189. In addition, (a) shows the distribution of scattered field intensity at  $\Omega=0.45$  in the region  $|x|<66.67a$  and  $-40a<y<93.33a$  with maximum intensity of 24.67.

To illustrate the importance of the upper sidewall, Fig. 1(b) shows an example of incomplete UDPS plates in which the upper sidewall is removed from Fig. 1(a) and UDPS's are filled in. Average transmittance of the TM mode over five cases including Fig. 1(b) is shown in Fig. 1(c) by the green line. As shown, the gap position and depth are almost identical to the blue line, indicating that gap structure is independent of the presence of the upper sidewall. However, the reflected electric field differs completely. We show in Fig. 1(b) the distributions of total electric-field intensity and energy flow at  $\Omega=0.40$ . The irregular presence of large intensity regions is shown by the yellow or red dots in front of the incomplete UDPS plate. This distribution demonstrates that the smoothness of sidewalls is an essential prerequisite for the UDPS plate to work as an ideal mirror. A recent independent report has indicated the importance of sidewalls for efficient transmission in the waveguide of PhC's.<sup>6</sup>

### III. UDPS MICROMIRRORS AND CAVITIES

Figure 1 illustrates the simple procedure for producing a UDPS plate of arbitrary shape: first decide the sidewall shape; then fill the surrounding region with UDPS's.

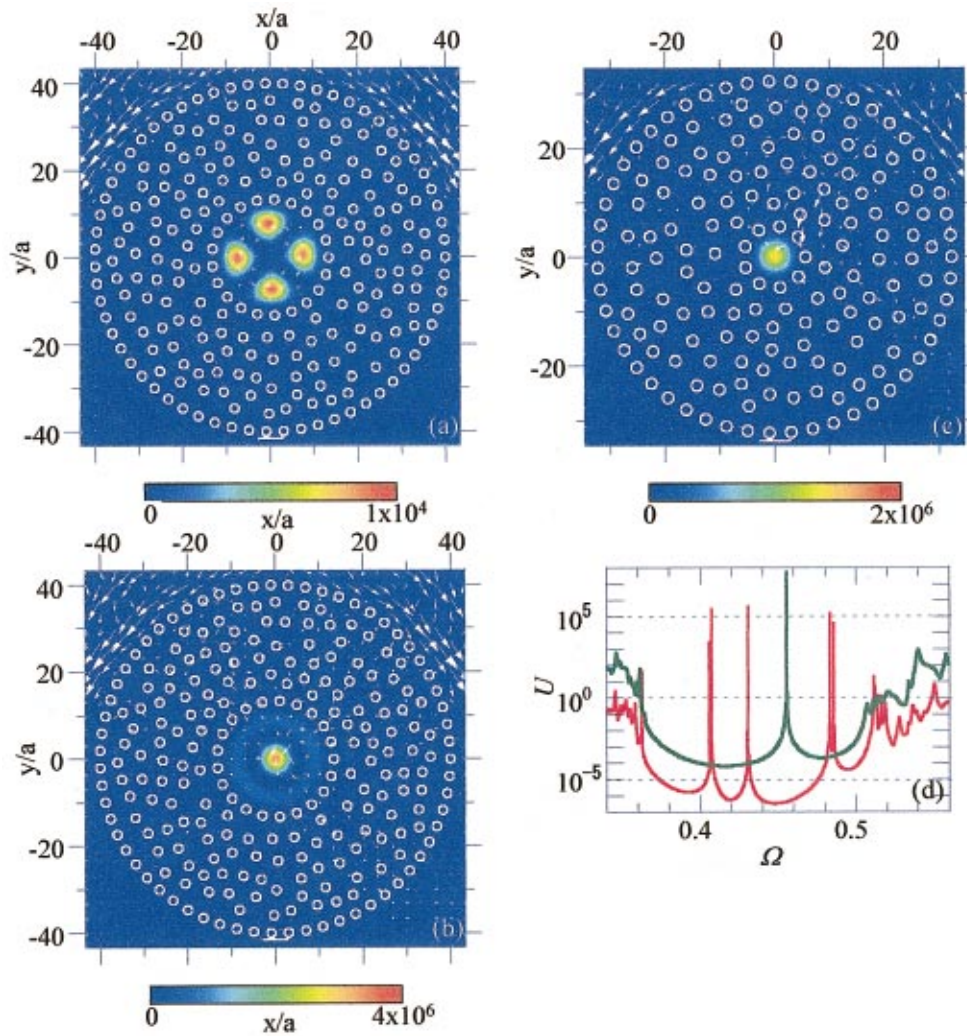


FIG. 3. (Color) (a)–(c) Circular cavities of inner radius  $R_{in}$  and outer radius  $R_{out}$ .  $R_{in}=13.33a$ ,  $R_{out}=40a$ , and  $V_f=0.169$  in (a) and (b) while  $R_{in}=5.66a$ ,  $R_{out}=32.33a$ , and  $V_f=0.171$  in (c). The plane wave of the TM mode is incident from the positive  $y$  axis. Also shown are distributions of total electric field intensity and energy flow at (a)  $\Omega=0.40586$ , (b)  $\Omega=0.43054$ , and (c)  $\Omega=0.45527$ . Maximum field intensity is (a)  $9.19 \times 10^3$ , (b)  $3.44 \times 10^6$ , and (c)  $1.42 \times 10^6$ . (d) Normalized energy  $U$  stored within cavities for the TM mode incidence. Red and green lines correspond to cavity (a) or (b) and (c), respectively.

Thereby, if we place periodic rods along a curve, we can produce a curved mirror of arbitrary shape and dimension. Figure 2(a) shows such an example in which the upper sidewall consists of equidistant rods (period= $4a$ ) on the parabola  $y=x^2/(4f)$  with  $f=16.67a$ . Here, we relaxed the UDPS condition  $D_{min} < |\mathbf{R}_l - \mathbf{R}_j|$  at right and left corners of upper sidewalls for simplicity of construction. Figure 2(b) shows the TM mode transmittance of plane wave incidence from positive  $y$  axis. Obviously, we observe the same PG with that in Fig. 1(c). Distribution of scattered electric field intensity at  $\Omega=0.45$  is also plotted in Fig. 2(a). The incident plane wave from positive  $y$  axis is collected reasonably well at the focal point ( $x=0$ ,  $y=f$ ) of a parabolic mirror in the geometrical optics. This fact indicates that the UDPS plate in Fig. 2(a) can be regarded as an almost ideal parabolic mirror.

Structural flexibility of the UDPS plate allows formation of a two-dimensional microcavity<sup>7</sup> of arbitrary shape with great ease. Figures 3(a)–(c) show circular cavities of inner and outer radius  $R_{in}$  and  $R_{out}$  between which we fill the UDPS's. The red line in Fig. 3(d) is a plot of normalized

electromagnetic energy  $U$  stored within the cavity in Figs. 3(a) or (b) for plane wave incidence of the TM mode from the positive  $y$  axis. Sharp peaks appear at  $\Omega=0.40586$ ,  $0.40702$ ,  $0.43054$ ,  $0.48318$ , and  $0.48580$  within PG's. These states are resonance states of the cavity. Corresponding values of quality factor  $Q$  at these peaks are  $1.49 \times 10^7$ ,  $1.37 \times 10^7$ ,  $2.56 \times 10^7$ ,  $2.95 \times 10^6$ , and  $3.77 \times 10^6$ .

Figures 3(a) and (b) also show distributions of total electric field intensity and energy flow at  $\Omega=0.40586$  and  $0.43054$ , respectively. The intensity distribution inside the cavity, shown in Fig. 3(a), has fourfold symmetry indicating that this peak corresponds to the state with azimuthal quantum number  $m=2$ , whereas that in Fig. 3(b) represents the state with  $m=0$ . The peak at  $\Omega=0.40702$  also shows fourfold symmetry, but its distribution is rotated by  $\pi/4$  from that in Fig. 3(a). This rotation is also evident for peaks at  $\Omega=0.48318$  and  $0.48580$ , which represent the resonance states with  $m=3$ . We can also observe smooth energy flow around the outer circle. This flow smoothness indicates that the outer sidewall plays the role of a circular mirror.

Resonance frequencies of the present circular cavity can be obtained approximately from the condition that the electric field vanishes at the inner boundary  $R=R_{in}$ . Corresponding size parameters are given in terms of the zeroes of the Bessel function  $J_m(j_{mk})=0$  ( $m \geq 0, k \geq 1$ ) as  $\Omega_{mk} = j_{mk}a/R_{in}$ . For  $R_{in} = 13.33a$ , we have nondegenerate level  $\Omega_{m=0,k=2} = 0.4140$ , and two doubly degenerate levels  $\Omega_{m=2,k=1} = 0.3852$  and  $\Omega_{m=3,k=1} = 0.4785$  within PG's. These values concur well with those in Fig. 3(d). To achieve better agreement, we simply reduce the cavity radius  $R_{in}$  by the order of rod radius  $a$ , which is consistent with the position of perfectly reflecting flat mirror in Fig. 1(a). The lift of degeneracy is caused by local nonuniformity of rod distribution in the UDPS's. The resonant field has exponentially decaying amplitude within the UDPS region. Because the field distributions at  $\Omega=0.40586$  and  $0.40702$  differ by  $\pi/4$  rotation, they are influenced by the difference of the rod distribution within the UDPS's, as shown in Fig. 3(a).

From a practical point of view, it is desirable to use single mode cavity with, say, the  $m=0$  and  $k=1$  mode. Such a single mode cavity can be designed easily using a UDPS cavity. If this mode is chosen to appear in the middle of a PG at, e.g.,  $\Omega=0.425$ , the cavity radius is determined as  $R_{in} = 5.66a$  because  $j_{m=0,k=1} = 2.405$  and  $R_{in} = j_{mk}a/\Omega_{mk}$ . A cavity of this size is plotted in Fig. 3(c), where UDPS plate thickness ( $R_{out} - R_{in}$ ) is identical to that of Figs. 3(a) and (b). Corresponding normalized internal energy is shown by the green line in Fig. 3(d) for plane wave incidence of the TM mode from positive  $y$  axis. As shown in that figure, only a single sharp peak appears at  $\Omega=0.45527$  with  $Q = 8.30 \times 10^6$ , shifted 7% from the predicted position. We also show in Fig. 3(c) the corresponding distributions of total electric field intensity and energy flow.

We will briefly discuss the origin of PG's in UDPS's. PG's are formed either by coherent interference of scattered waves from periodic rods like Bragg diffraction in x rays or by bonding and antibonding states of Mie resonance within each rod that are similar to electronic band gaps in semiconductors. The latter are formed by local interaction. Therefore they are not as easily smeared out by fluctuations in position and radius of rods as in the former case. Therefore we con-

clude that PG's of UDPS's result from interaction of Mie resonance states. However, an important difference exists between electrons and photons: resonance wave functions of photons are not localized exponentially. Rather, they decay in inverse power and have a long-range nature. This long-range nature of wave functions is responsible for formation of PG's in UDPS's which do not require even a short-range order. Consequently, UDPS's can acquire tremendous structural flexibility that is free from either long-range or short-range ordering.

#### IV. SUMMARY

We have proposed a two-dimensional photonic material called a UDPS plate. It is a combination of smooth sidewalls and UDPS filling material. The UDPS plate allows the design of arbitrarily curved mirrors of wavelength size and circular microcavity of requested resonance frequencies. Because the UDPS cavity shape is not limited to that of a circle, the UDPS plate provides an intriguing research field of various microcavities of complicated shapes. A detailed discussion of various characteristics of UDPS plates will be undertaken in future studies.

#### ACKNOWLEDGMENTS

This work was supported by a Grant-in-Aid for Scientific Research from the Ministry of Education, Culture, Sports, Science, and Technology. One author (H.M.) particularly thanks R. Ohkawa for his continued encouragement and inspiration.

- <sup>1</sup>J. D. Joannopoulos, P. R. Villeneuve, and S. Fan, *Nature (London)* **386**, 143 (1997).
- <sup>2</sup>A. Mekis, J. C. Chen, I. Kurland, Shanhui Fan, Pierre R. Villeneuve, and J. D. Joannopoulos, *Phys. Rev. Lett.* **77**, 3787 (1996).
- <sup>3</sup>S.-Y. Lin, E. Chow, V. Hietala, P. R. Villeneuve, and J. D. Joannopoulos, *Science* **282**, 274 (1998).
- <sup>4</sup>H. Miyazaki, M. Hase, H. T. Miyazaki, Y. Kurokawa, and N. Shinya, *Phys. Rev. B* **67**, 235109 (2003).
- <sup>5</sup>H. A. Yousif and S. Kohler, *J. Opt. Soc. Am. A* **5**, 1085 (1988).
- <sup>6</sup>K.-C. Kwan, X. Zhang, Z.-Q. Zhang, and C. T. Chan, *Appl. Phys. Lett.* **82**, 4414 (2003).
- <sup>7</sup>E. Yablonovitch, T. J. Gmitter, R. D. Meade, A. M. Rappe, K. D. Brommer, and J. D. Joannopoulos, *Phys. Rev. Lett.* **67**, 3380 (1991).